

Efficient adaptive step size control for exponential integrators

Pranab Jyoti Deka, Lukas Einkemmer

Department of Mathematics, University of Innsbruck, A-6020 Innsbruck, Austria

Abstract

Traditional step size controllers make the tacit assumption that the cost of a time step is independent of the step size. This is reasonable for explicit and implicit integrators that use direct solvers. In the context of exponential integrators, however, an iterative approach, such as Krylov methods or polynomial interpolation, to compute the action of the required matrix functions is usually employed. In this case the assumption of constant cost is not valid. This is, in particular, a problem for higher-order exponential integrators, which are able to take relatively large time steps based on accuracy considerations. In this paper, we consider an adaptive step size controller for exponential Rosenbrock methods that determines the step size based on the premise of minimizing computational cost. The largest allowed step size, given by accuracy considerations, merely acts as a constraint. We test this approach on a range of nonlinear partial differential equations. Our results show significant improvements (up to a factor of 4 reduction in the computational cost) over the traditional step size controller for a wide range of tolerances.

Keywords: automatic step size selection, adaptive step size controller, exponential integrators, exponential Rosenbrock methods, Leja interpolation

1. Introduction

Solving time dependent partial differential equations (PDEs) numerically is an important task in many fields of science and engineering. Consequently, improvements in numerical algorithms have contributed greatly to better understand a range of natural phenomena and such methods are essential in many industrial settings. Faster numerical methods, in this context, allow us to perform simulations with increased fidelity, e.g. increasing the number of grid points, including more physical effects, etc.

While explicit numerical methods are suitable for some problems, for many PDEs a large efficiency improvement can be attained by using implicit time integrators. Consequently, such methods have attained much interest and many software packages have been written to facilitate the use of such methods by practitioners, see e.g. [16, 17]. More recently, so-called exponential Rosenbrock integrators have been introduced [21]. We refer to the review article [20] for more details. This class of methods linearizes the partial differential equation and then treats a matrix function representing the linear part using Krylov iteration, Leja interpolation, or Taylor methods. Similar to implicit integrators, exponential Rosenbrock methods can take much larger time steps than explicit methods. However, the fact that such methods do not approximate the linear part of the equation (except for the error in the iterative scheme) allows them, in many situations, to take even larger time steps. Moreover, these methods do not suffer from the dichotomy between good behavior on the negative real axis (where the stability function is expected to decay) and on the imaginary axis (where the stability function should have unit magnitude) that afflicts implicit integrators. Because of this, exponential integrators have been used extensively and demonstrated to be superior compared to implicit methods in several situations, see e.g. [18, 22, 5, 11, 9, 8].

To facilitate the use of software packages based on these integrators by practitioners, it is desirable to free the user from explicitly choosing the time step size. Ideally, the user would only prescribe a tolerance and the numerical algorithm would then select an appropriate step size. To accomplish this, so-called (automatic) step size controllers are used in conjunction with an error estimator. Ideally, this also frees the user from verifying the accuracy of the simulations (by numerical convergence studies or similar means). Step size controllers can increase the computational efficiency by allowing the software to adaptively increase and/or decrease the step size during the course of the simulation.

Almost all step size controllers are predicated on the assumption that the largest possible step size should be selected. Thus, the step size is chosen such that the error committed exactly matches the tolerance specified by

Email addresses: pranab.deka@uibk.ac.at (Pranab Jyoti Deka), lukas.einkemmer@uibk.ac.at (Lukas Einkemmer)

the user (in practical implementations often a safety factor is imposed to avoid frequent step size rejection). This is a reasonable assumption for explicit Runge–Kutta methods, where the computational cost is independent of the step size. However, this approach is also used in many implicit and exponential software packages. For example, the implicit RADAU5 code [16, Chap. IV.8] and the implicit multistep based CVODE code [17] use this approach. These implicit (or exponential) methods require an iterative solution of a linear system or the iterative computation of the action of certain matrix functions. This is commonly done by iterative methods. However, the number of iterations required is quite sensitive to the properties of the matrix. Smaller time step sizes reduce the magnitude of the largest eigenvalue of the matrix, which in turn reduces the number of iterations required per time step. This means that reducing the time step size below what is dictated by the specified tolerance can actually result in an increase in performance, thereby invalidating the assumption that the cost of a time step is independent of the step size.

None of the widely employed step size controllers are able to exploit this fact. This is problematic for two reasons. First, it reduces the computational efficiency by taking time steps size that do not yield optimal performance. Second, such step size controllers often do not show a monotonous increase in cost as the tolerance decreases. Thus decreasing the tolerance can actually (sometimes drastically) reduce the run-time required for the simulations. Such behaviour is observed in a range of test problems [22, 23, 18] as well as for problems that stem from more realistic physical models [11, 2, 26]. The problem with this behaviour is that the user of the software is once again tasked with tuning the parameters of the method (i.e. decreasing the tolerance until the run-time is minimized). Thus, this largely negates the utility of an automatic step size controller. This behaviour can be observed for exponential integrators as well as implicit Runge–Kutta methods, BDF methods, and implicit-explicit (IMEX) methods.

While all of the considerations made above are valid for implicit schemes just as well as for exponential integrators, the issues raised become even more important for exponential integrators. The reason being that exponential integrators, especially for problems where nonlinear effects are relatively weak, are often able to take even larger time steps than implicit integrators. Thus, exponential integrators when used in conjunction with a traditional step size controller are more likely to operate in a regime that is problematic.

In the context of ordinary differential equations, the importance of considering variations in cost (as a function of the time step size) has been recognized in [15]. There analytically derived estimates of the cost are used. Obtaining a good a priori estimate of the cost is often extremely difficult for (especially nonlinear) PDEs. In the context of approximating matrix exponentials by polynomial interpolation at Leja points (a precursor for exponential integrators), a procedure to determine the optimal step size based on a backward error analysis has been proposed [4]. This approach can be very effective but requires certain information on the spectrum of the matrix under consideration. This information is not easily obtained in a matrix free implementation and, for nonlinear PDEs, can change from one time step to the next. In addition, it is well known that for such an approach, the number of iterations is overestimated and early truncation criteria have to be used to obtain optimal performance.

In [12], an adaptive step size controller has been introduced that explores the space of admissible step sizes (i.e. step sizes that satisfy the tolerance) dynamically during the simulation and adapts the step size based on the measured cost. This has the advantage that no prior estimates of the cost are needed. In fact, no information of the iterative scheme used or the hardware where the simulation is run, enters the algorithm. Only the computational cost of the previously conducted time steps is used. It was shown in [12] that, for a number of implicit Runge–Kutta methods, this approach reduces the overall computational cost significantly and results in a monotonic relation of the computational effort with the run time.

The goal of the this paper is to consider an adaptive step size controller for exponential integrators and to investigate its performance. This controller is an extension of the method described in [12] to exponential integrators. As mentioned above, using adaptive step size control is particularly important in the case of exponential integrators. We demonstrate that the developed controller performs well, that is, it increases computational efficiency and removes the non-monotonous behaviour observed in the traditional approach to step size control. We also compare the performance of the adaptive step size controller to the implicit approach proposed in [12] and find that the present approach can yield improvements in performance of up to an order of magnitude.

The paper is structured as follows. An introduction to exponential integrators and our implementation is presented in section 2. In section 3, the principle of the proposed step size controller is presented. The performance of this step size controller is then analyzed for some nonlinear problems in section 4. We conclude our study in section 5.

2. Exponential Integrators

In this section, we provide an introduction to exponential integrators and Leja interpolation that we use to compute the action of the resulting matrix-vector products. We refer the reader to [20] for more details. Let us

consider the initial value problem

$$\frac{\partial u}{\partial t} = f(u), \quad u(t=0) = u^0, \quad (1)$$

where $u = u(x, t)$ in 1D, $u = u(x, y, t)$ in 2D, and $f(u)$ is some nonlinear function of u (usually depends on spatial derivatives of u). Linearizing Eq. 1 about u^n , the starting point for a given time step, we get

$$\frac{\partial u}{\partial t} = \mathcal{J}(u^n)u + \mathcal{F}(u),$$

where $\mathcal{J}(u)$ is the Jacobian of the nonlinear function $f(u)$ and $\mathcal{F}(u) = f(u) - \mathcal{J}(u)u$ is the nonlinear remainder. We use exponential Rosenbrock (EXPRB) methods [19] to solve equations of this form. The simplest of the EXPRB methods, known as the *exponential Rosenbrock–Euler* method, is given by

$$u^{n+1} = u^n + \Delta t \varphi_1(\mathcal{J}(u^n)\Delta t)f(u^n), \quad (2)$$

where the superscripts n and $n+1$ indicate the time steps. The $\varphi_l(z)$ functions are defined by the recursive relation

$$\varphi_{l+1}(z) = \frac{1}{z} \left(\varphi_l(z) - \frac{1}{l!} \right), \quad l \geq 1$$

with

$$\varphi_0(z) = e^z$$

which corresponds to the matrix exponential. The exponential Rosenbrock–Euler method is second-order accurate and only needs the action of one matrix function per time step. Moreover, an error estimator for Eq. 2 has been developed by [7]. For the second order accuracy to hold, it is crucial that the Jacobian is used. In fact, integrators that replace the Jacobian by an arbitrary linear operator, require more stages to obtain a given order. These methods are referred to as either exponential Runge–Kutta methods or exponential time differencing methods. We will only consider exponential Rosenbrock methods in this paper. Many higher order variants of this idea are available in the literature, see e.g. [20, 25, 24]. Of particular interest in this work are higher order embedded schemes that, similar to embedded Runge–Kutta methods, are a pair of exponential integrators with same internal stages but different order. The difference between these two methods is then used to cheaply obtain an error estimate for adaptive step size control.

In this work, we use the fourth-order (EXPRB43) scheme with a third-order error estimator, presented in [21] and the Butcher tableau of which can be found in [20]. The two internal stages are given by a_n and b_n , and the third and fourth-order solutions are given by Eq. 3 and 4 respectively. The difference between these two solutions gives an error estimate of order three.

$$\begin{aligned} a^n &= u^n + \varphi_1 \left(\frac{1}{2} \mathcal{J}(u^n) \Delta t \right) f(u^n) \frac{1}{2} \Delta t \\ b^n &= u^n + \varphi_1(\mathcal{J}(u^n)\Delta t) f(u^n) \Delta t \\ &\quad + \varphi_1(\mathcal{J}(u^n)\Delta t) (\mathcal{F}(a^n) - \mathcal{F}(u^n)) \Delta t \end{aligned}$$

$$\begin{aligned} u^{n+1} &= u^n + \varphi_1(\mathcal{J}(u^n)\Delta t) f(u^n) \Delta t \\ &\quad + \varphi_3(\mathcal{J}(u^n)\Delta t) (-14\mathcal{F}(u^n) + 16\mathcal{F}(a^n) - 2\mathcal{F}(b^n)) \Delta t \end{aligned} \quad (3)$$

$$\begin{aligned} u^{n+1} &= u^n + \varphi_1(\mathcal{J}(u^n)\Delta t) f(u^n) \Delta t \\ &\quad + \varphi_3(\mathcal{J}(u^n)\Delta t) (-14\mathcal{F}(u^n) + 16\mathcal{F}(a^n) - 2\mathcal{F}(b^n)) \Delta t \\ &\quad + \varphi_4(\mathcal{J}(u^n)\Delta t) (36\mathcal{F}(u^n) - 48\mathcal{F}(a^n) + 12\mathcal{F}(b^n)) \Delta t \end{aligned} \quad (4)$$

2.1. Leja interpolation

The main computational effort required in an exponential integrator is to evaluate the action of the matrix functions φ_k . Similar to the treatment of linear solves in implicit schemes, iterative methods are commonly used to treat the large matrices resulting from the spatial discretization of PDEs. Krylov subspace methods, methods based on polynomial interpolation, and Taylor methods are the most common options. A comparison of many of these methods has been conducted in [1, 3]. In this work we will exclusively use interpolation at Leja points. However, the developed adaptive step size controller is expected to work equally well for other strategies.

An effective way of computing the action the matrix exponential and the φ_k functions is interpolation at Leja points [6]. Here, we present a synopsis of the algorithm that we use in our implementation (following [3]). Appropriately placing the interpolation points requires the spectral properties of the matrix. Let us suppose that the eigenvalues of the matrix A satisfy

$$\alpha \leq \operatorname{Re} \sigma(A) \leq \nu \leq 0, \quad -\beta \leq \operatorname{Im} \sigma(A) \leq \beta,$$

where $\sigma(A)$ denotes the spectrum of A ; α and ν are the smallest and largest real eigenvalues respectively, and β is the largest, in modulus, imaginary eigenvalue. The values of α , ν , and β can be obtained by Gershgorin's disk theorem.

One can then construct an ellipse, with semi-major axis a and semi-minor axis b , consisting of all the eigenvalues of the matrix A . For real eigenvalues, let c be the midpoint of the ellipse and γ be one-fourth the distance between the two foci of the ellipse. For the matrix exponential, we interpolate the function $\exp(c + \gamma\xi)$ on pre-computed Leja points (ξ) in the interval $[-2, 2]$.

The n^{th} term of the interpolation polynomial $p(z)$ is defined as

$$\begin{aligned} p_n(z) &= p_{n-1}(z) + d_n y_{n-1}(z), \\ y_n(z) &= y_{n-1}(z) \times \left(\frac{z - c}{\gamma} - \xi_m \right), \end{aligned}$$

where the d_i correspond to the divided differences of the function $\exp(c + \gamma\xi)$. For imaginary eigenvalues, one can interpolate the function $\exp(c + \gamma\xi)$ on the interval $i[-2, 2]$. To interpolate φ_k functions on Leja points, one can simply replace $\exp(c + \gamma\xi)$ with $\varphi_k(c + \gamma\xi)$.

In this study, we approximate the action of the φ_k functions by interpolating them as a polynomial on Leja points. The preference for Leja points over the well-known Chebyshev points can be attributed to the fact that the interpolation of a polynomial at $m + 1$ Chebyshev nodes necessitates the re-computation of the matrix-vector products at the previously computed m nodes. However, Leja points can be generated in a sequence: using $m + 1$ Leja points needs only one extra computation, and the computation at the previous m nodes can be reused.

3. Adaptive Step Size Controller

To conduct automatic step size control, an error estimate is essential to ensure that the local error is below the user-specified tolerance. Embedded schemes, which share the internal stages, can be efficiently used as error estimators (with only a small increase in computation cost). Richardson extrapolation is one of the other commonly used error estimator.

The widely used traditional step size controller uses the largest step size (with a safety factor) that satisfies the prescribed tolerance. This implicitly assumes that the cost of each step size is independent of the step size Δt . This is true for explicit methods or implicit methods that solve the corresponding linear systems using direct methods. Let us suppose that the error incurred in the n^{th} time step is $e^n = D(\Delta t^n)^{(p+1)}$, where p is the order of the method used and D is some constant. The tolerance specified by the user is tol . The optimal step size, for $(n + 1)^{\text{th}}$ time step, is given by $\text{tol} = D(\Delta t^{n+1})^{(p+1)}$. Eliminating D , we get

$$\Delta t^{n+1} = \Delta t^n \times \left(\frac{\text{tol}}{e^n} \right)^{1/(p+1)}$$

This simple formula can be interpreted as a P controller. The mathematical analysis is, in fact, based on this observation (see, for example, [14, 13, 27, 28]). A PI controller has also been proposed in [14]. These local step size controllers form the backbone of most time integration packages. For example, the RADAU5 code [16, Chap. IV.8] employs a variant of the PI controller, while the multistep based CVODE code [17] and [10] uses a variant of the P controller.

For iterative methods (in the context of implicit or exponential time integrators), the computational cost depends on the step size; the larger the step size, the larger the number of iterations needed for the integration to converge. As such, it is not always beneficial to choose the largest possible step size. Taking this into consideration, [12] developed an adaptive step size controller where the step size is chosen based on the computational expenses at the previous time steps. This step size controller is engineered to select step sizes to minimize the computational cost (which might be substantially smaller than the one selected by the traditional controller).

This approach works as follows: the step size is adjusted in accordance with the computational cost (c) per unit time step

$$c^n = \frac{i^n}{\Delta t^n}$$

where i^n is the runtime or a proxy such as the number of matrix-vector products needed in that time step. The goal of this step size controller is to adjust the step size such that $c^n \rightarrow \min$. We consider the logarithm of the step size $\Delta T^n = \ln \Delta t^n$ and the computational cost $C^n(\Delta T^n) = \ln c^n(\Delta t^n)$. One-dimensional gradient descent is implemented to estimate T^{n+1}

$$T^{n+1} = T^n - \gamma \nabla C^n(T^n),$$

where γ is the learning rate. The gradient can be approximated by taking finite differences

$$\nabla C^n(T^n) \approx \frac{C^n(T^n) - C^n(T^{n-1})}{T^n - T^{n-1}}$$

This implies that we are not allowed to choose a constant time step size, i.e. $T^n \neq T^{n-1}$. Operating with a constant time step size would not provide any information on how the time step should be changed to optimize performance. It is worth noting that $C^{n-1}(T^n)$ corresponds to the cost of a step size (Δt^n) starting from t^{n-1} whereas $C^n(T^n)$ is the cost incurred for the same step size (Δt^n) starting from t^n . During the time integration of a problem, we automatically obtain $C^{n-1}(T^{n-1})$ and not $C^n(T^{n-1})$. Therefore, we write the gradient as

$$\begin{aligned} \nabla C^n(T^n) &\approx \frac{C^n(T^n) - C^n(T^{n-1})}{T^n - T^{n-1}} \\ &= \frac{C^n(T^n) - C^{n-1}(T^{n-1})}{T^n - T^{n-1}} + \frac{C^{n-1}(T^{n-1}) - C^n(T^{n-1})}{T^n - T^{n-1}} \\ &\approx \frac{C^n(T^n) - C^{n-1}(T^{n-1})}{T^n - T^{n-1}}, \end{aligned}$$

where in the last step we have assumed that C^n varies slowly as a function of n . This yields

$$T^{n+1} = T^n - \gamma \frac{C^n(T^n) - C^{n-1}(T^{n-1})}{T^n - T^{n-1}}.$$

Taking exponentials on both sides of the equation, we get

$$\Delta t^{n+1} = \Delta t^n \exp(-\gamma \Delta), \quad \Delta = \frac{\ln c^n - \ln c^{n-1}}{\ln \Delta t^n - \ln \Delta t^{n-1}}.$$

Here, γ is a free parameter, which can possibly depend on c and τ . Choosing γ to be a constant would be the easiest choice. However, this has two major disadvantages. First, we can not guarantee that $\Delta t^n \neq \Delta t^{n-1}$, which would lead to numerical problems in computing Δ . Second, in some situations the controller can yield prohibitively large changes in step size. We, therefore, compute the new step size Δt^{n+1} as follows

$$\Delta t^{n+1} = \Delta t^n \times \begin{cases} \lambda & \text{if } 1 \leq s < \lambda, \\ \delta & \text{if } \delta \leq s < 1, \\ s := \exp(-\alpha \tanh(\beta \Delta)) & \text{otherwise.} \end{cases}$$

The parameter α acts as a constraint on the maximal allowed step size change: the maximum change in step size is given by $\exp(\pm\alpha)$. The parameter β determines how strongly the controller reacts to a change in the cost. The factors λ and δ have been incorporated to ensure that the step size changes by at least $\lambda \Delta t$ or $\delta \Delta t$ depending on whether Δt needs to be increased or decreased for minimizing the cost. They are chosen in such a way that results in non-trivial changes in the step size if Δ is close to 0.

These parameters, (α , β , λ , and δ) have been numerically optimized for the linear diffusion-advection equation and an implicit Runge–Kutta scheme for a range of values of N , η , and tol. This step size controller has been designed with two variants: (i) *Non-penalized* variant: the aforementioned parameters have been chosen to incur the minimum possible cost, (ii) *Penalized* variant: if the traditional controller performs better than the non-penalized variant, a penalty is charged on the proposed controller. This penalty has been imposed to trade off the enhanced performance of the proposed controller (where it performs better) with an acceptable amount of diminished performance (where it performs worse than the traditional controller). The numerical optimization yields the following set of parameters

$$\begin{aligned} \text{Non-penalized} \quad & \alpha = 0.65241444 \quad \beta = 0.26862269 \quad \lambda = 1.37412002 \quad \delta = 0.64446017 \\ \text{Penalized} \quad & \alpha = 1.19735982 \quad \beta = 0.44611854 \quad \lambda = 1.38440318 \quad \delta = 0.73715227 \end{aligned}$$

The improved performance of this controller for both implicit schemes [12] and exponential integrators (as we will see in this paper) further shows the generality of the approach. In particular, this is emphasized as the parameters that have been obtained for a linear PDE generalize well to nonlinear problems for a variety of numerical methods.

It is worth noting that the proposed step size controller is designed solely to minimize the computational cost and does not take into account the error incurred during the time integration. As such, we need to take the minimum of the step sizes given by the traditional and the proposed step size controller

$$\Delta t^{n+1} = \min \left(\Delta t_{\text{proposed}}^{n+1}, \Delta t_{\text{traditional}}^{n+1} \right)$$

This ensures that, in addition to satisfying the accuracy requirements set by the user, the controller minimizes the computational cost (by choosing a smaller time step size) whenever possible.

In the context of exponential integrators, there is an additional detail that needs to be taken care of: the computation of the Leja interpolation to the prescribed tolerance. In some situations, especially if relatively large step sizes are chosen, the polynomial interpolation might fail to converge within a reasonable number of iterations. If this is the case for any of the internal stages of the exponential Rosenbrock scheme, we reject the step and use the traditional controller to determine a smaller step size.

4. Numerical results

In this section, we investigate the performance of the proposed step size controller and compare it with the traditional controller using the embedded EXPRB43 scheme for a number of nonlinear problems. We present a detailed explanation of how the step size controller can improve the performance of exponential Rosenbrock methods in practice.

4.1. Viscous Burgers' Equation

The one-dimensional viscous Burgers' equation (conservative form) reads

$$\frac{\partial u}{\partial t} = \frac{1}{2}\eta \frac{\partial u^2}{\partial x} + \frac{\partial^2 u}{\partial x^2},$$

where periodic boundary conditions are imposed in $[0, 1]$. The Péclet number (η) is a measure of the relative strength of advection to diffusion. Higher values of η indicate advection-dominated scenarios whereas lower values of η imply diffusion-dominated cases. Periodic boundary conditions are imposed on $[0, 1]$. The initial condition is

$$u(x, t = 0) = 1 + \exp \left(1 - \frac{1}{1 - (2x - 1)^2} \right) + \frac{1}{2} \exp \left(-\frac{(x - x_0)^2}{2\sigma^2} \right)$$

with $x_0 = 0.9$ and $\sigma = 0.02$.

We wish to test our step size controller in diffusion as well as advection dominated cases. If η is small (diffusion dominated), then the Gaussian part is dynamically smeared out, and $u(x, t)$ is slowly advected over a significant amount of time. If η is large (advection dominated), the solution experiences rapid advection and the Gaussian is smeared out after a long time. We choose the final time of the integration to be $t = 10^{-2}$. This means that for any value of η , a fixed amount of diffusion is inherently introduced in the simulations. For the space discretization, we consider a third-order upwind scheme for advection and the second-order centered difference scheme for diffusion (see 5).

The work-precision diagram is shown in Fig. 1. The computational cost incurred, in our case, measured by the number of matrix-vector products, is plotted as a function of the user-specified tolerance. The blue curves correspond

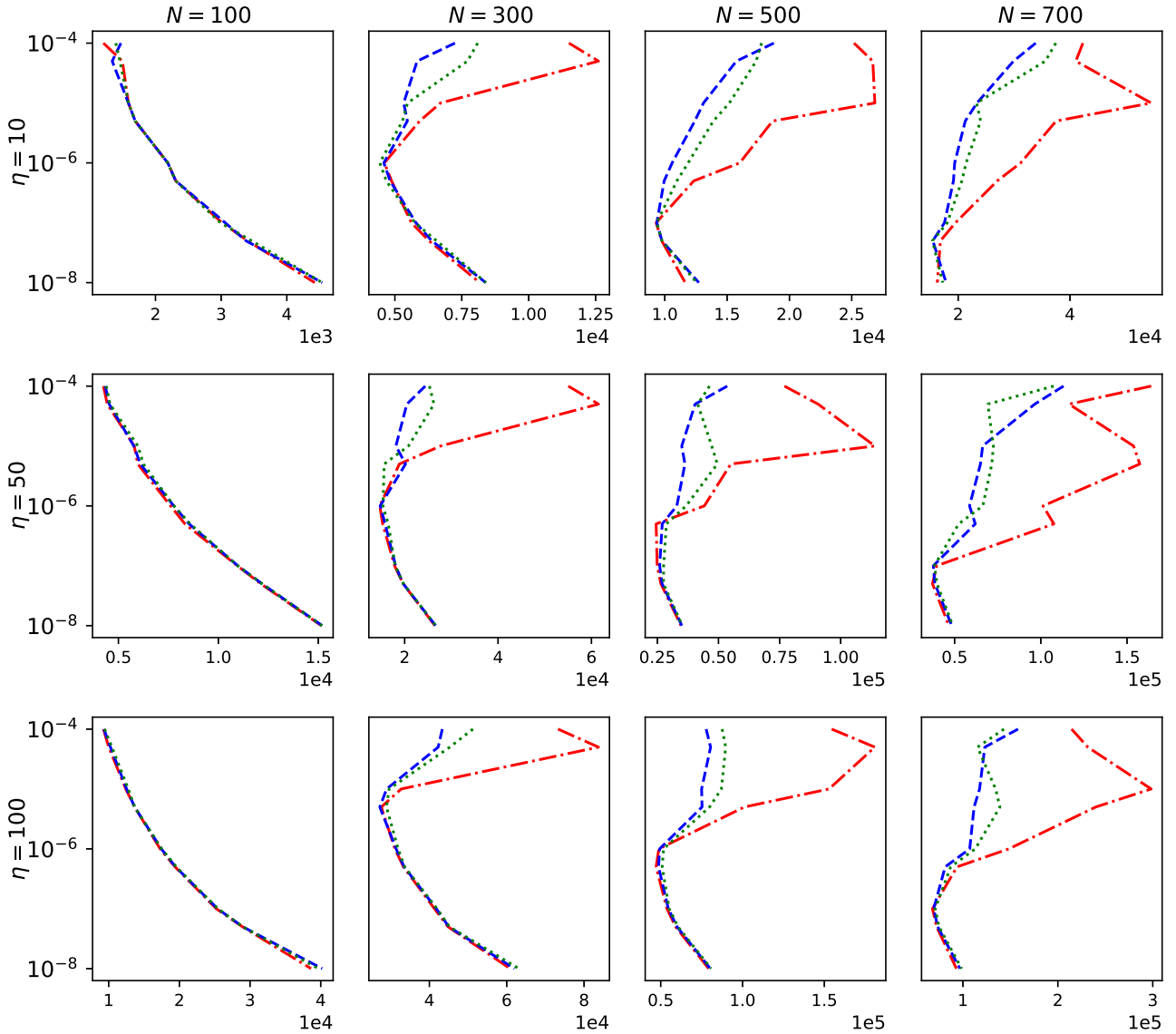


Figure 1: Figure shows the number of matrix-vector products (i.e computational cost) vs. tolerance for the 1D viscous Burgers' equation for different values of η and N . The red dashed-dotted lines correspond to the traditional controller, green dotted lines the penalized variant, and the blue dashed lines represents the non-penalized variant of the proposed step size controller.

to the non-penalized version of the proposed controller, the green ones refer to the penalized variant, and the red lines represent the traditional controller. The performance of the proposed step size controller is similar to the traditional controller for $N = 100$ for all values of η . As the number of grid points is increased, one can see that the proposed step size controller performs significantly better in the lenient to intermediate tolerance regime. This is true for all values of η . Maximum speedups up to a factor of 2.5 are observed. To illustrate how this performance improvement is achieved, we compare, in Fig. 2, the step size used at each time step during the simulation with the proposed controller (blue curves) with the largest possible step size (constrained only by the accuracy requirements) estimated by the traditional controller (red curves). We see that the step sizes estimated by the proposed controller are smaller than what would be possible based purely on accuracy constraints. This justifies the fundamental principle of the proposed step size controller; i.e., multiple small step sizes incur less computational effort than a single large step size. It can also be seen in Fig. 2 that the proposed step size controller continuously varies the step size to find the step size that minimizes the computational cost. For stringent tolerances, the traditional controller already yields small step sizes. Further reduction in step sizes would only result in an increased number of time steps leading to an increase in the computational cost. All in all, the step size controller (both non-penalized and penalized variants) has superior performance for a reasonably wide range of tolerances for advection as well as diffusion dominated cases.

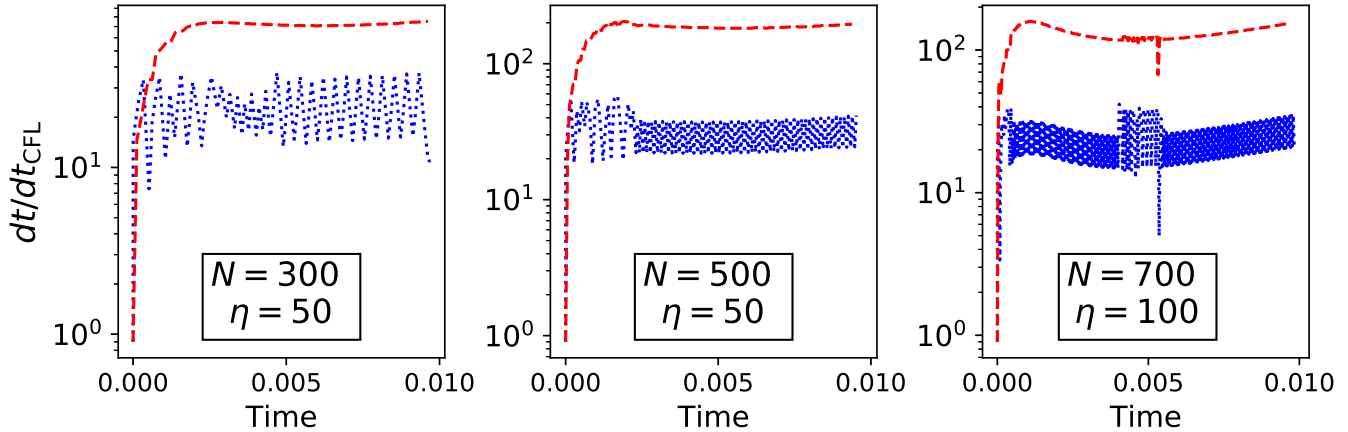


Figure 2: Figure compares the step sizes used during the simulation with the non-penalized variant of the proposed controller (blue dotted lines) with the step sizes yielded by the traditional controller for tolerance, $\text{tol} = 10^{-4}$. It can clearly be seen that for the proposed controller in most of the integration interval the step sizes are significantly reduced which results in improved performance.

Moreover, as the step sizes are further reduced by the proposed controller, the solution is, in fact, more accurate. This is in addition to the reduced computational cost. It also largely avoids the inverse C-shaped curve observed for the traditional controller. We also note that the proposed step size controller is notably efficient in the intermediate tolerance regime which is relevant for most practical applications.

Using an embedded method is not the only way to obtain an error estimate for automatic step size control. Richardson extrapolation, while usually being more expensive, has the advantage that it can be applied to any existing time integrator. The proposed step size controller is independent of how the error estimate is obtained. To illustrate this, we apply it to the third-order solution of EXPRB43 with Richardson extrapolation as an error estimator. The results are shown in Fig. 3, along with a comparison with the embedded EXPRB43 and the explicit embedded Runge–Kutta–Fehlberg 45 (RKF45) schemes. One can clearly see that the proposed step size controller works reasonably well in this case, although the embedded Rosenbrock scheme significantly outperforms the Richardson extrapolation method, as would be expected. It is worth noting that the ‘shape’ of the curves is fairly similar for both these methods. This tells us that the embedded scheme and the Richardson extrapolation have similar changes in behaviour with the increase or decrease in tolerance. The explicit embedded scheme RKF45 (fourth-order solution) is over an order of magnitude more expensive than the corresponding exponential integrator counterparts. Any reduction in step size, compared to the traditional controller, would only result in an increased number of time steps leading to an increased computational cost. As such, the performance of the traditional controller and the proposed controller is the same for this integrator.

Fig. 4 compares the step sizes (non-penalized variant of the proposed step size controller) for the embedded EXPRB43 scheme and Richardson extrapolation with the third-order solution. One can see that the step sizes for the embedded scheme are, in general, larger than the step sizes for the Richardson extrapolation. The increased number of time steps is likely to be an additional contribution to the expenses of the Richardson extrapolation method. For $N = 700; \eta = 10$, the step sizes for the embedded scheme are similar to that of Richardson extrapolation in the lenient tolerance regime ($\text{tol} = 10^{-4}$: red lines). As such, the computational costs are somewhat similar. As the tolerance is reduced, the step sizes allowed by Richardson extrapolation decrease substantially, thereby incurring more cost ($\text{tol} = 10^{-7}$ and 10^{-8} : blue and green lines respectively). Similar arguments can be used to explain the other cases as well. The step sizes permitted by the explicit RKF45, depicted in Fig. 5, are significantly smaller (roughly 1 - 2 orders of magnitude) than EXPRB43. Consequently, this incurs a hefty computational cost and has the worst performance out of the three schemes presented here.

Now, we compare the performance of the exponential Rosenbrock approach with implicit and explicit integrators. Table 1 compares the performance of the non-penalized variant of the proposed step size controller for the embedded EXPRB43 scheme with the two-stage third-order singly diagonally implicit Runge-Kutta (SDIRK23) scheme used in [12] (with the same controller) and the RKF45 scheme. It is evident that the embedded Rosenbrock method has superior performance compared to the other two; up to an order of magnitude over the implicit integrator and up to two orders of magnitude over the explicit integrator can be observed for some configurations. Similar results have been obtained for the inviscid Burgers’ equation and the porous medium equation that are discussed in the following sections.

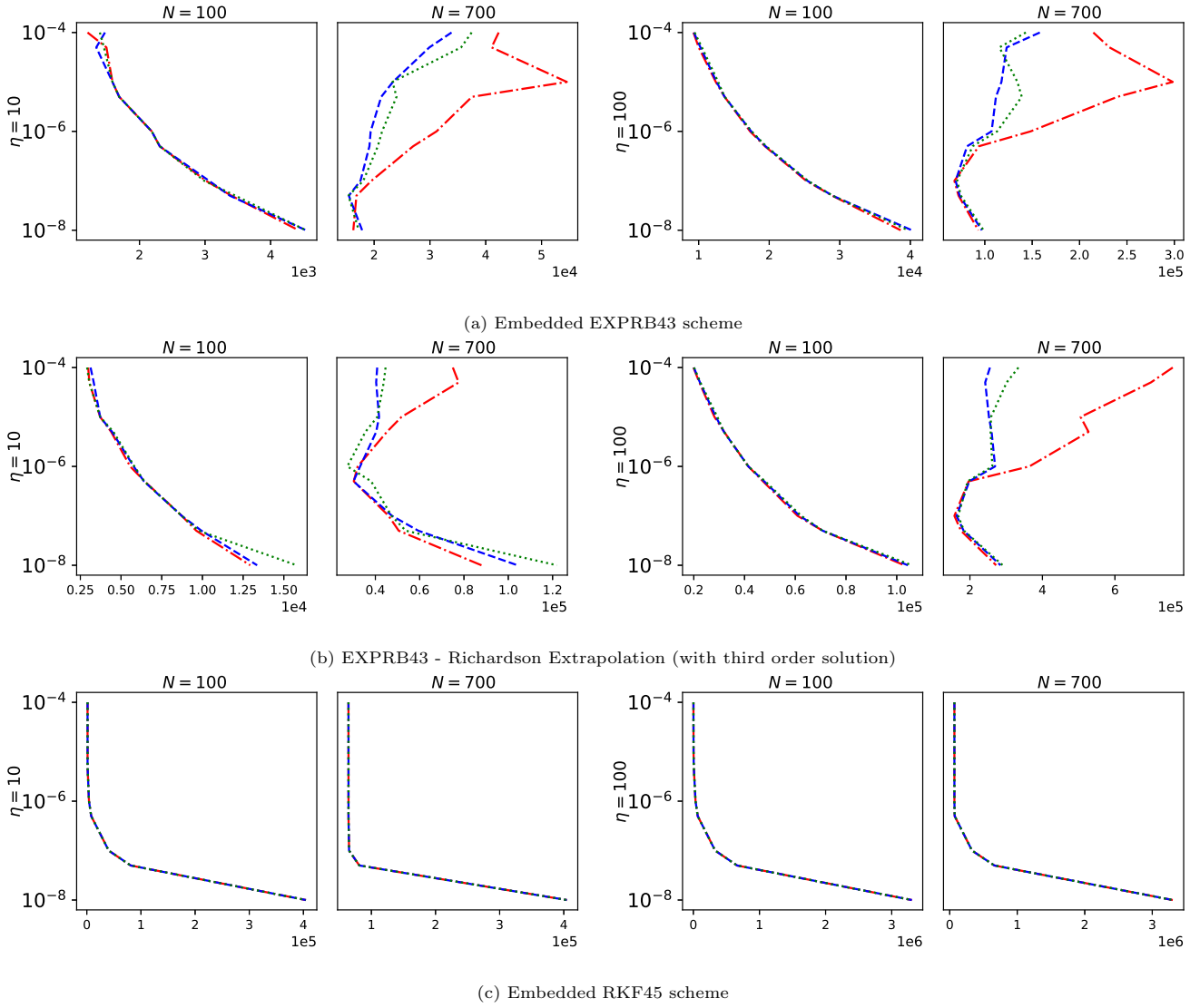


Figure 3: Comparison of the number of matrix-vector products (i.e computational cost) vs. tolerance for the 1D viscous Burgers' equation for the embedded EXPRB43 scheme (top row), Richardson extrapolation with the third-order solution of this embedded scheme, and the explicit RKF45 integrator. Here we consider two different values of η and N each. The red dashed-dotted lines correspond to the traditional controller, green dotted lines the penalized variant, and the blue dashed lines represents the non-penalized variant of the proposed step size controller.

Next, we test our step size controller on the two-dimensional viscous Burgers' equation:

$$\frac{\partial u}{\partial t} = \frac{1}{2} \left(\eta_x \frac{\partial u^2}{\partial x} + \eta_y \frac{\partial u^2}{\partial y} \right) + \frac{\partial^2 u}{\partial x^2} + \frac{\partial^2 u}{\partial y^2},$$

where η_x and η_y are the components of the Péclet number along X and Y directions, respectively. Periodic boundary conditions are considered on $[0, 1] \times [0, 1]$. The initial condition is chosen to be

$$u(x, y, t = 0) = 1 + \exp \left(1 - \frac{1}{1 - (2x - 1)^2} - \frac{1}{1 - (2y - 1)^2} \right) + \frac{1}{2} \exp \left(\frac{-(x - x_0)^2 - (y - y_0)^2}{2\sigma^2} \right)$$

with $x_0 = 0.9$, $y_0 = 0.9$, and $\sigma = 0.02$.

The work-precision diagram is shown in Fig. 6. The proposed step size controller has a similar performance compared to the one-dimensional case. With the increase in the number of grid points, the proposed controller shows a large improvement in performance (up to a factor of 3) for lenient tolerances for the different values of η_x and η_y considered here.

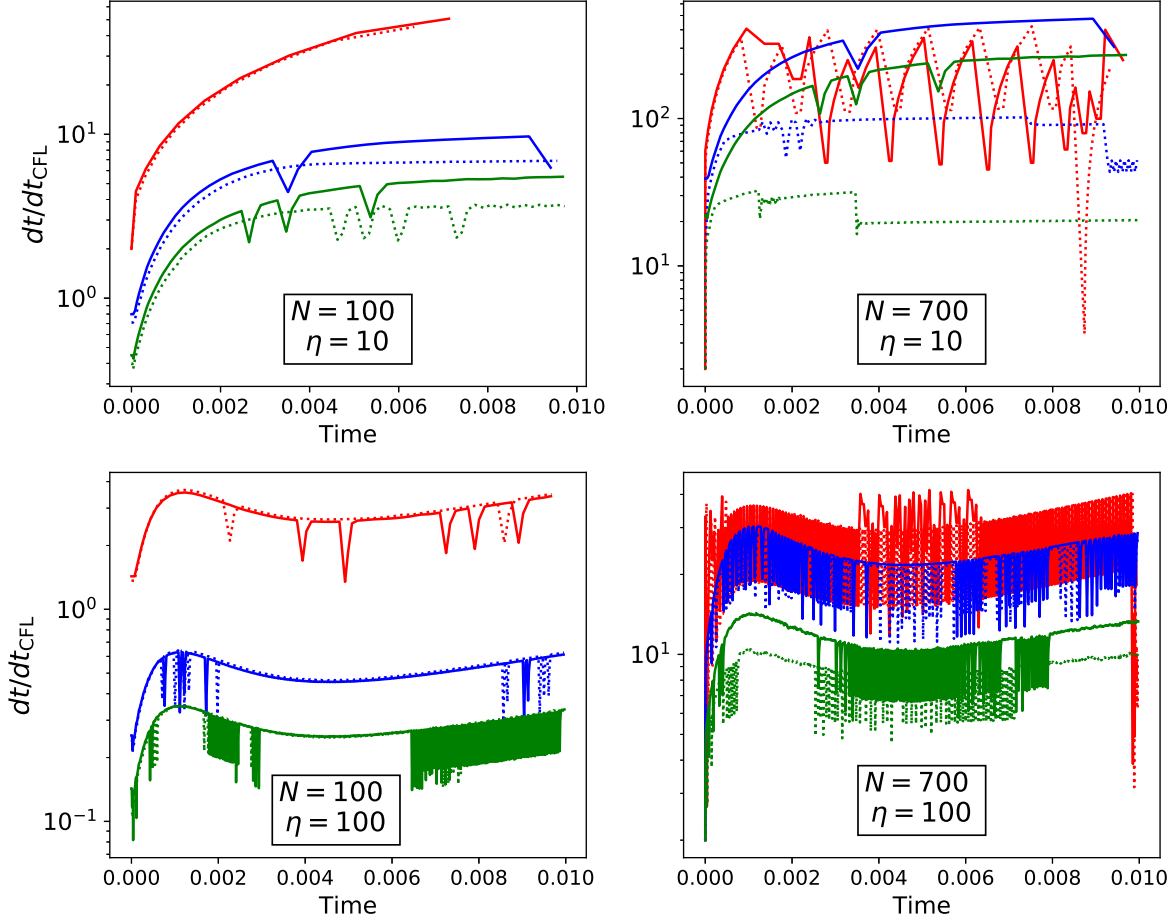


Figure 4: Figure illustrates the step sizes (normalized to the CFL time) for four different combinations of N and η . The solid lines represent the embedded EXPRB43 scheme and the dotted lines represent Richardson extrapolation with the third-order solution. The colours indicate different tolerances: 10^{-4} (red), 10^{-7} (blue), and 10^{-8} (green). The step sizes are shown for the non-penalized variant of the proposed step size controller.

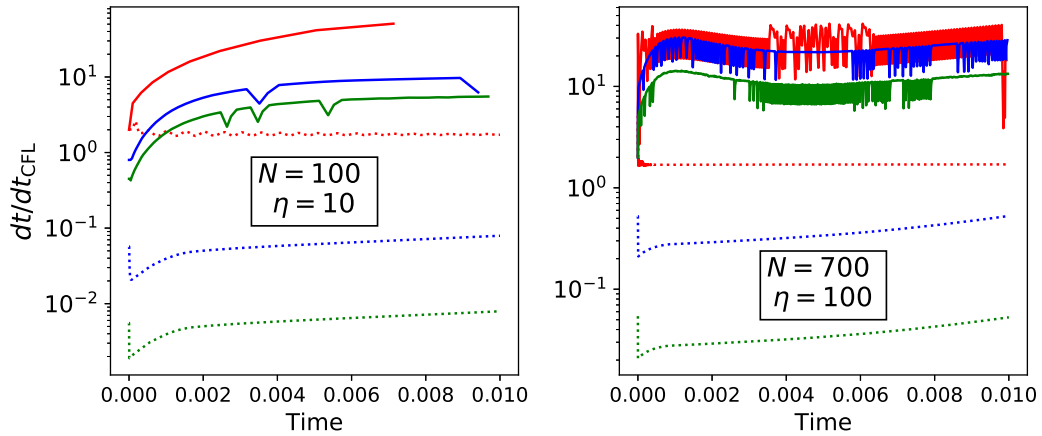


Figure 5: Figure illustrates the step sizes (normalized to the CFL time) for two different combinations of N and η . The solid lines represent the embedded EXPRB43 scheme and the dotted lines represent the explicit RKF45. The colours indicate different tolerances: 10^{-4} (red), 10^{-7} (blue), and 10^{-8} (green). The step sizes are shown for the non-penalized variant of the proposed step size controller.

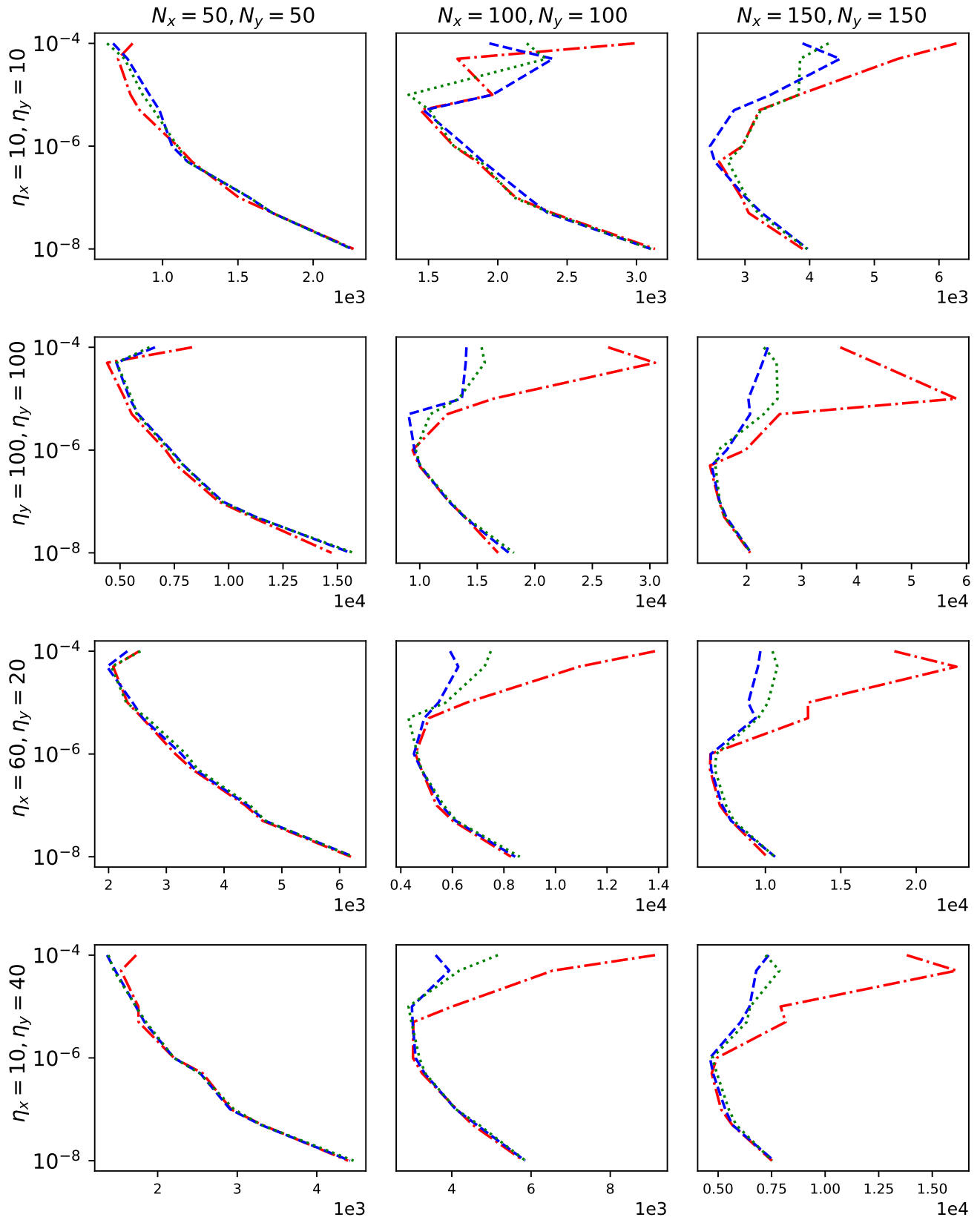


Figure 6: Figure shows the number of matrix-vector products (i.e computational cost) vs. tolerance for the 2D viscous Burgers' equation. The values of N_x , N_y , η_x , and η_y are varied. The red dashed-dotted lines correspond to the traditional controller, green dotted lines the penalized variant, and the blue dashed lines represents the non-penalized variant of the proposed step size controller.

Parameters	SDIRK23	EXPRB43	RKF45
$N = 100, \eta = 10$	$10^4 - 3 \cdot 10^4$	$10^3 - 4 \cdot 10^3$	$1.5 \cdot 10^3 - 4 \cdot 10^5$
$N = 100, \eta = 100$	$5 \cdot 10^4 - 2 \cdot 10^5$	$2 \cdot 10^4 - 3 \cdot 10^4$	$6 \cdot 10^4 - 4 \cdot 10^5$
$N = 700, \eta = 10$	$5 \cdot 10^4 - 1.5 \cdot 10^5$	$10^4 - 4 \cdot 10^4$	$2 \cdot 10^3 - 3.5 \cdot 10^6$
$N = 700, \eta = 100$	$5 \cdot 10^5 - 1.5 \cdot 10^6$	$10^5 - 2 \cdot 10^5$	$7 \cdot 10^4 - 3.5 \cdot 10^6$

(a) Viscous Burgers' Equation

Table 1: A quantitative comparison of the computational cost incurred by EXPRB43, RKF45, and SDIRK23 (used in [12]) for the viscous Burgers' equation and the range of tolerance considered in this study is shown.

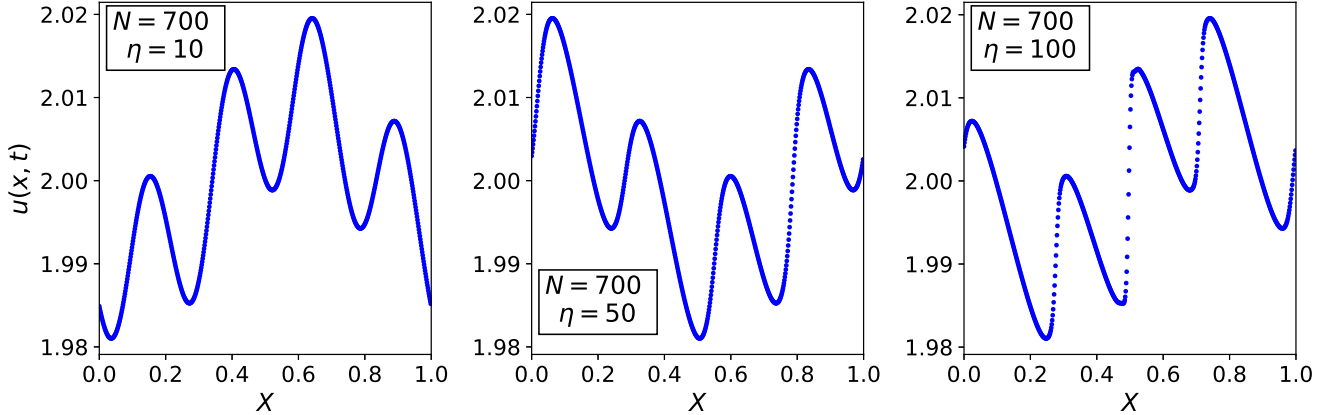


Figure 7: Figure shows the solution at the final time $t = 3.25\eta \times 10^{-2}$ for the inviscid Burgers' equation. It can be seen that the solution yields progressively steeper gradients for large values of η . Further increase in the simulation time would result in a shock.

4.2. Inviscid Burgers' Equation

We consider the conservative form of the inviscid Burgers' equation

$$\frac{\partial u}{\partial t} = \frac{1}{2} \frac{\partial u^2}{\partial x}.$$

Periodic boundary conditions are considered on $[0, 1]$ and the initial condition is given by

$$u(x, t = 0) = 2 + \epsilon_1 \sin(\omega_1 x) + \epsilon_2 \sin(\omega_2 x + \phi)$$

with $\epsilon_1 = \epsilon_2 = 10^{-2}$, $\omega_1 = 2\pi$, $\omega_2 = 8\pi$, and $\phi = 0.3$. The simulations are carried out until $t = 3.25\eta \times 10^{-2}$, where η is some constant. The distribution at the final time, for different values of η , is depicted in Fig. 7. A change in η corresponds to a change in the final time of the simulation. As time progresses, the gradients start becoming progressively sharper. The solution gradually approaches a shock wave. It is worth noting that this effect is more prominent in cases with larger values of N . This is due to the fact that the numerical diffusion decreases as the number of grid points are increased leading to increasingly steeper gradients.

The work-precision diagram is illustrated in Fig. 8. It can be seen that the proposed step size controller 'flattens out' the zig-zag shape of the curves yielded by the traditional controller to a large extent. This yields a significant improvement over the traditional controller, especially in the lenient to medium tolerance range. Performance improvements of up to a factor of 4 are observed. Both step size controllers have some difficulty dealing with large values of η and large N , i.e. with very sharp gradients in the solution.

We extend our 1D model into 2 dimensions. The two-dimensional inviscid Burgers' equation is given by

$$\frac{\partial u}{\partial t} = \frac{1}{2} \left(\frac{\partial u^2}{\partial x} + \frac{\partial u^2}{\partial y} \right).$$

Periodic boundary conditions are considered on $[0, 1] \times [0, 1]$ and the initial condition is

$$u(x, y, t = 0) = 2 + \epsilon_1 \sin(\omega_1 x) + \epsilon_2 \sin(\omega_2 x + \phi) + \epsilon_1 \sin(\omega_1 y) + \epsilon_2 \sin(\omega_2 y + \phi)$$

with $\epsilon_1 = \epsilon_2 = 10^{-2}$, $\omega_1 = 2\pi$, $\omega_2 = 8\pi$, and $\phi = 0.3$.

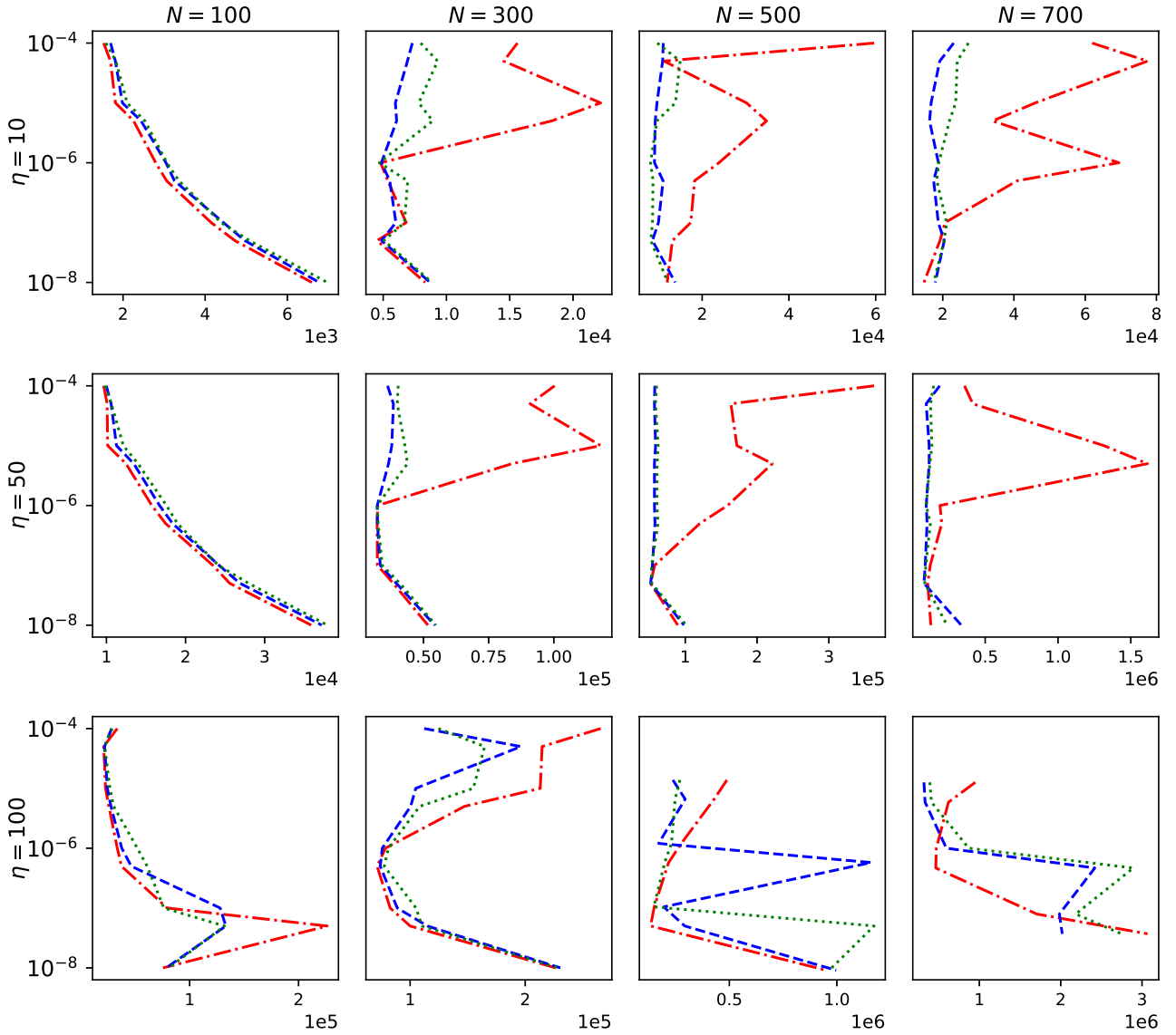


Figure 8: Figure shows the number of matrix-vector products (i.e computational cost) vs. tolerance for the 1D inviscid Burgers' equation for different values of η and N . The red dashed-dotted lines correspond to the traditional controller, green dotted lines the penalized variant, and the blue dashed lines represents the non-penalized variant of the proposed step size controller.

The corresponding work-precision diagram is shown in Fig 9. Once again, we see features similar to the one-dimensional case. The curves are flattened-out for lenient tolerances signifying a significant improvement over the traditional controller. For stringent tolerances, both controllers work well. It can also be seen that an increase in the number of grid points correlates with an enhanced performance of the proposed controller for a wider range of tolerance. This is in agreement with what we have seen for the 1D case.

4.3. Porous Medium Equation

The last example considered is the porous medium equation with linear advection. The one dimensional equation reads

$$\frac{\partial u}{\partial t} = \eta \frac{\partial u}{\partial x} + \frac{\partial^2 u^m}{\partial x^2},$$

where we have chosen $m = 2$ and η is the Péclet number. As usual, periodic boundary conditions are considered on $[0, 1]$ and the initial condition is given by

$$u(x, t = 0) = 1 + \Theta(x_1 - x) + \Theta(x - x_2).$$

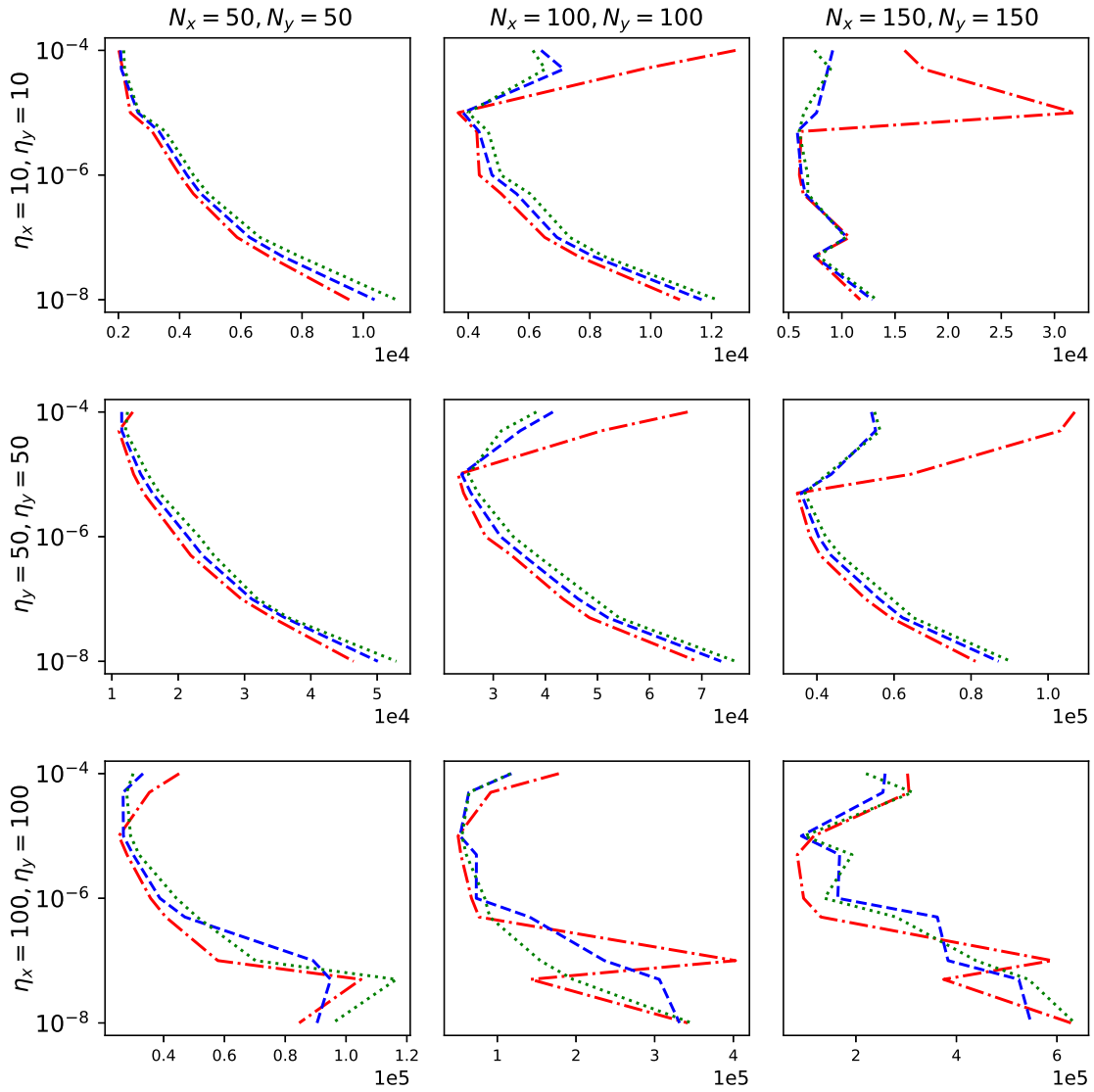


Figure 9: Figure shows the number of matrix-vector products (i.e computational cost) vs. tolerance for the 2D inviscid Burgers' equation. The values of N_x , N_y , η_x , and η_y are varied. The red dashed-dotted lines correspond to the traditional controller, green dotted lines the penalized variant, and the blue dashed lines represents the non-penalized variant of the proposed step size controller.

Here, $x_1 = 0.25$, $x_2 = 0.6$, and Θ is the Heaviside function. This corresponds to a rectangle, i.e. a discontinuous initial value. The nonlinear diffusivity dynamically smears out this discontinuity as the system evolves in time and results in a smooth solution. The simulations are carried out up to a final time of $t = 10^{-2}$.

The corresponding results are shown in Fig. 10. The performance of the proposed controller is similar to that of the traditional controller for $\eta = 10$ in the lenient to medium tolerance range. As η increased, one can appreciate the significant reduction in computational cost (up to a factor of 4) for both variants of the proposed controller and a broad range of tolerance. For stringent tolerance, the traditional controller marginally outperforms the proposed controller. This can be attributed to the fact that for stringent tolerances, any further reduction in step size, as prescribed by the traditional controller, leads to an increased number of time steps.

Finally, we consider the porous medium equation in two dimensions

$$\frac{\partial u}{\partial t} = \eta_x \frac{\partial u}{\partial x} + \eta_y \frac{\partial u}{\partial y} + \frac{\partial^2 u^m}{\partial x^2} + \frac{\partial^2 u^m}{\partial y^2},$$

where $m = 2$ and η_x and η_y are the components of the Péclet number along the X and Y directions, respectively. Periodic boundary conditions are considered on $[0, 1] \times [0, 1]$. The initial condition is given by

$$u(x, y, t = 0) = 1 + \Theta(x_1 - x) + \Theta(x - x_2) + \Theta(y_1 - y) + \Theta(y - y_2),$$

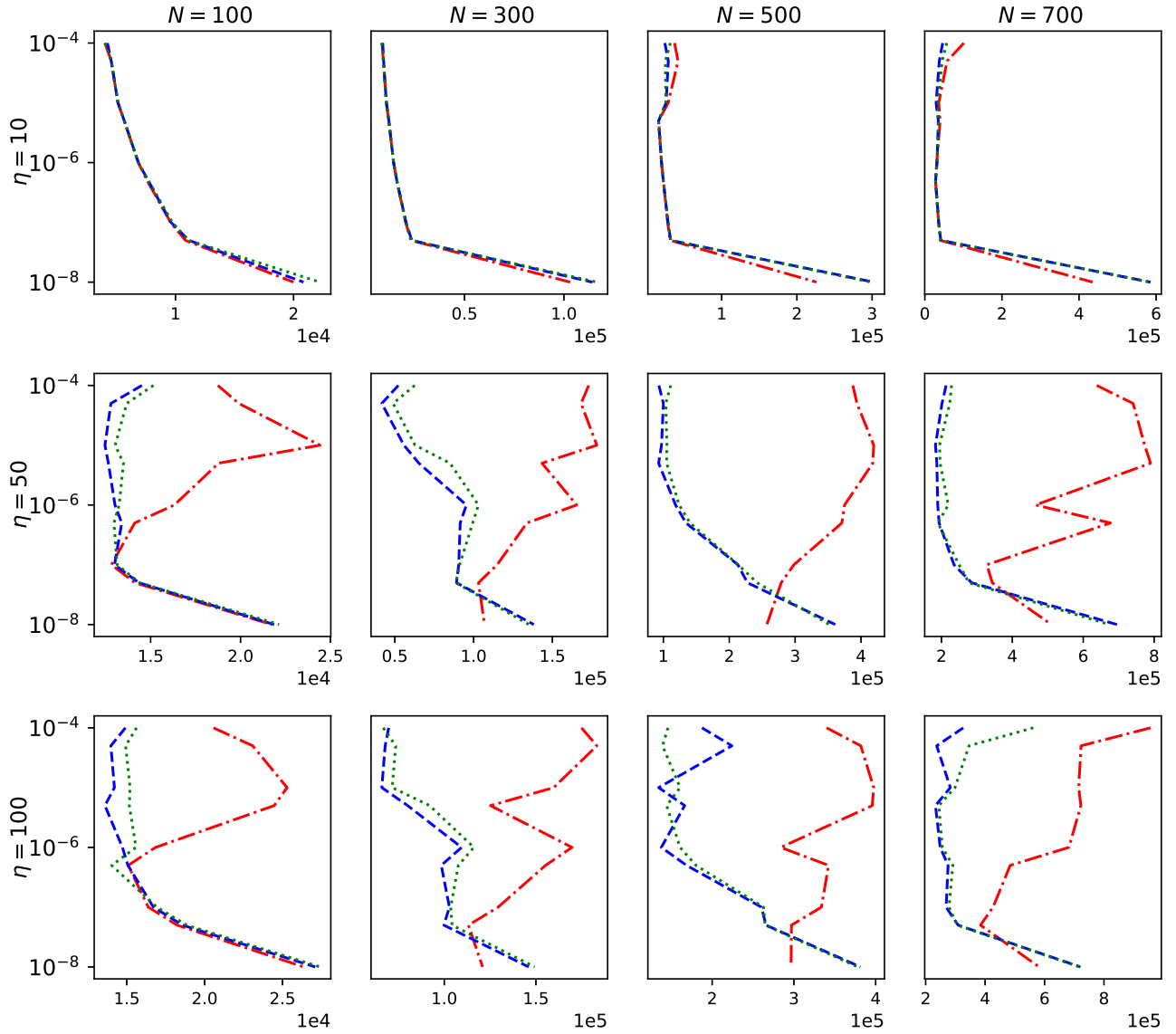


Figure 10: Figure shows the number of matrix-vector products (i.e computational cost) vs. tolerance for the 1D porous medium equation for different values of η and N . The red dashed-dotted lines correspond to the traditional controller, green dotted lines the penalized variant, and the blue dashed lines represents the non-penalized variant of the proposed step size controller.

where $x_1 = y_1 = 0.25$, $x_2 = y_2 = 0.6$, and Θ is the Heaviside function. This initial state corresponds to a cuboid. Similar to the 1D case, the nonlinear diffusion rapidly smears out the discontinuity resulting in a progressively smoother solution.

The work-precision diagram for the 2D scenario (Fig. 11) shows that the proposed step size controller improves the performance in all the considered configurations. In addition, the curves are flattened-out to a large extent.

5. Conclusions

In this manuscript, we have considered an adaptive step size controller for exponential Rosenbrock methods. The fundamental principle of this step size controller is that the step size should be chosen to minimize computational cost, constrained by the maximal allowed time step; the latter is set by accuracy considerations. This allows the step size controller to adaptively decrease the step size which can drastically improve the performance. Specifically, we have used an embedded exponential Rosenbrock method, EXPRB43, which has a third-order error estimate. The implementation of this time integrator involves polynomial interpolation at Leja points to compute the action of certain matrix functions. A comprehensive comparison of the proposed step size controller with the traditional

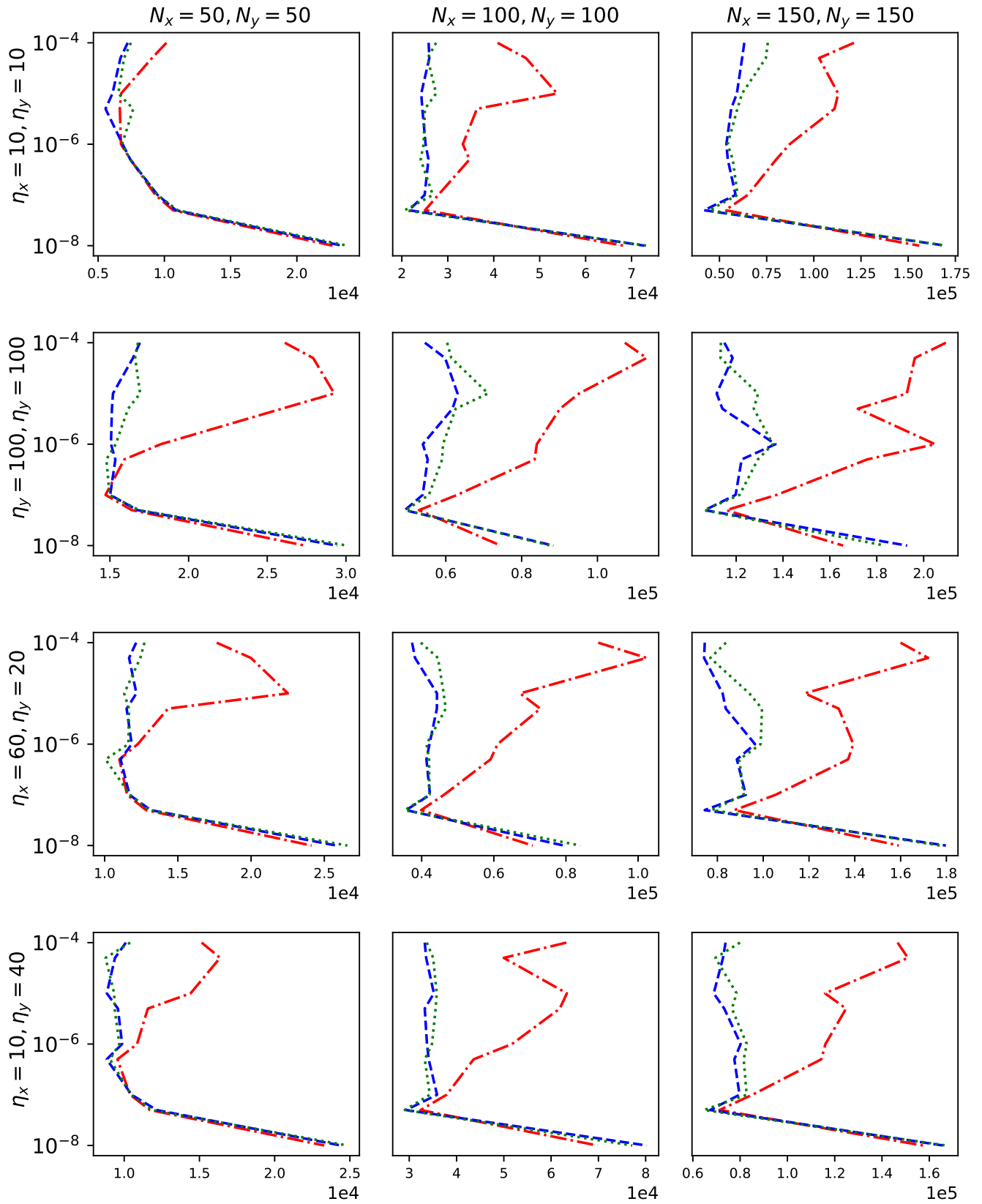


Figure 11: Figure shows the number of matrix-vector products (i.e computational cost) vs. tolerance for the 2D porous medium equation. The values of N_x , N_y , η_x , and η_y are varied. The red dashed-dotted lines correspond to the traditional controller, green dotted lines the penalized variant, and the blue dashed lines represents the non-penalized variant of the proposed step size controller.

controller has been presented for different values of the Peclet number, the number of the grid points, and the user-specified tolerance for the various equations under consideration. We summarize our results as follows:

- The proposed step size controller has superior performance (compared to the traditional controller) for almost all configurations considered here. This is particularly true in the lenient to medium tolerance regime. Arguably, equations in physics and astrophysics are solved up to accuracy within this range of tolerances. The zig-zag curves, yielded by the traditional controller, are flattened out. This exemplifies the use of such a step size controller in practice.
- Multiple small step sizes, in many situations, do indeed incur less computational effort than a single large step size and we have seen that the proposed step size controller can effectively exploit this fact.
- It has been observed that the curves for the work-precision diagrams have similar ‘shapes’ in 1D and 2D. This indicates the reliability and effectiveness of the proposed controller.
- Comparisons with explicit (RKF45) and implicit (SDIRK23) schemes have shown that the exponential Rosenbrock method outperforms both these classes of integrators by a significant margin.
- We recommend the non-penalized variant of the step size controller as it shows improved performance in almost all configurations considered.

This study has been performed for a set of representative but relatively simple problems. In future work, we will implement this step size controller as part of a software package and test it for more realistic scenarios. A typical example would be the propagation of fluids or particles in the interstellar or intergalactic medium in 3D. This may include a combination of linear and/or nonlinear advection and diffusion coupled to other physical processes like dispersion, collisions, etc.

Acknowledgements

This work is supported by the Austrian Science Fund (FWF)—project id: P32143-N32.

Spatial Discretization

We use the third order upwind scheme to discretize the advective term which is given by

$$\frac{\partial u}{\partial x} \approx \frac{-u_{i+2} + 6u_{i+1} - 3u_i - 2u_{i-1}}{6 \Delta x} \quad (.1)$$

The primary advantage of this scheme is that it introduces less numerical diffusion. The structure or features of the physical parameter under consideration is preserved to a large extent. The diffusive term is discretized using the second-order centered difference scheme

$$\frac{\partial^2 u}{\partial x^2} \approx \frac{u_{i+1} - 2u_i + u_{i-1}}{\Delta x^2} \quad (.2)$$

References

- [1] L. Bergamaschi, M. Caliari, A. Martinez, and M. Vianello. Comparing Leja and Krylov approximations of large scale matrix exponentials. In *Proc. ICCS 2006*, pages 685–692. Springer, 2006.
- [2] D. S. Blom, P. Birken, H. Bijl, F. Kessels, A. Meister, and A. H. van Zuijlen. A comparison of Rosenbrock and ESDIRK methods combined with iterative solvers for unsteady compressible flows. *Adv. Comput. Math.*, 42(6):1401–1426, 2016.
- [3] M. Caliari, P. Kandolf, A. Ostermann, and S. Rainer. Comparison of software for computing the action of the matrix exponential. *BIT Numer. Math.*, 54:113 – 128, 2014.
- [4] M. Caliari, P. Kandolf, A. Ostermann, and S. Rainer. The Leja method revisited: Backward error analysis for the matrix exponential. *SIAM J. Sci. Comput.*, 38(3):A1639–A1661, 2016.
- [5] M. Caliari and A. Ostermann. Implementation of exponential Rosenbrock-type integrators. *Appl. Numer. Math.*, 59(3-4):568–581, 2009.

- [6] M. Caliari, M. Vianello, and L. Bergamaschi. Interpolating discrete advection–diffusion propagators at leja sequences. *J. Comput. Appl. Math.*, 172(1):79 – 99, 2004.
- [7] Marco Caliari and Alexander Ostermann. Implementation of exponential rosenbrock-type integrators. *Appl. Numer. Math.*, 59(3):568 – 581, 2009.
- [8] N. Crouseilles, L. Einkemmer, and J. Massot. Exponential methods for solving hyperbolic problems with application to collisionless kinetic equations. *J. Comput. Phys.*, 420:109688, 2020.
- [9] N. Crouseilles, L. Einkemmer, and M. Prugger. An exponential integrator for the drift-kinetic model. *Comput. Phys. Commun.*, 224:144–153, 2018.
- [10] S. Eckert, H. Baaser, D. Gross, and O. Scherf. A BDF2 integration method with step size control for elastoplasticity. *Comput. Mech*, 34(5):377–386, 2004.
- [11] L. Einkemmer, M. Tokman, and J. Loffeld. On the performance of exponential integrators for problems in magnetohydrodynamics. *J. Comput. Phys.*, 330:550–565, 2017.
- [12] Lukas Einkemmer. An adaptive step size controller for iterative implicit methods. *Appl. Numer. Math.*, 132:182 – 204, 2018.
- [13] K. Gustafsson. Control-theoretic techniques for stepsize selection in implicit Runge-Kutta methods. *ACM Trans. Math. Software*, 20(4):496–517, 1994.
- [14] K. Gustafsson, M. Lundh, and G. Söderlind. A PI stepsize control for the numerical solution of ordinary differential equations. *BIT Numer. Math.*, 28(2):270–287, 1988.
- [15] K. Gustafsson and G. Söderlind. Control strategies for the iterative solution of nonlinear equations in ODE solvers. *SIAM J. Sci. Comput.*, 18(1):23–40, 1997.
- [16] E. Hairer and G. Wanner. *Solving Ordinary Differential Equations II, Stiff and Differential-Algebraic Problems*. Springer Berlin Heidelberg, 1996.
- [17] A. C. Hindmarsh and R. Serban. User Documentation for cvode v2.9.0. https://computation.llnl.gov/sites/default/files/public/cv_guide.pdf, 2016.
- [18] M. Hochbruck, C. Lubich, and H. Selhofer. Exponential integrators for large systems of differential equations. *SIAM J. Sci. Comput.*, 19(5):1552–1574, 1998.
- [19] M. Hochbruck and A. Ostermann. Explicit integrators of rosenbrock-type. *Oberwolfach Rep.*, 3:1107 – 1110, 2006.
- [20] M. Hochbruck and A. Ostermann. Exponential integrators. *Acta Numer.*, 19:209 – 286, 2010.
- [21] M. Hochbruck, A. Ostermann, and J. Schweitzer. Exponential Rosenbrock-type methods. *SIAM J. on Numer. Anal.*, 47(1):786–803, 2009.
- [22] J. Loffeld and M. Tokman. Comparative performance of exponential, implicit, and explicit integrators for stiff systems of ODEs. *J. Comput. Appl. Math.*, 241:45–67, 2013.
- [23] V. T. Luan, M. Tokman, and G. Rainwater. Preconditioned implicit-exponential integrators (IMEXP) for stiff PDEs. *J. Comput. Phys.*, 335:846–864, 2017.
- [24] Vu Thai Luan and D. Michels. Explicit exponential rosenbrock methods and their application in visual computing. *arXiv:1805.08337*, 2018.
- [25] Vu Thai Luan and Alexander Ostermann. Parallel exponential rosenbrock methods. *Comput. Math. with Appl.*, 71(5):1137 – 1150, 2016.
- [26] M. Narayanamurthi, P. Tranquilli, A. Sandu, and M. Tokman. EPIRK-W and EPIRK-K time discretization methods. *arXiv:1701.06528*, 2017.
- [27] G. Söderlind. Automatic control and adaptive time-stepping. *Numer. Algorithms*, 31(1-4):281–310, 2002.
- [28] G. Söderlind. Time-step selection algorithms: Adaptivity, control, and signal processing. *Appl. Numer. Math.*, 56(3-4):488–502, 2006.